EEET ECOLOGICAL ENGINEERING & ENVIRONMENTAL TECHNOLOGY

Ecological Engineering & Environmental Technology 2024, 25(4), 172–187
https://doi.org/10.12912/27197050/183636
ISSN 2719-7050, License CC-BY 4.0

Received: 2024.02.01
Accepted: 2024.02.14
Published: 2024.02.25

Assessing Impact of Land Use/Land Cover Dynamic on Urban Climate Change in a Semi-Arid Region – Case Study of Agadir City (Morocco)

Ijjou Idoumskine[1*], Ali Aydda[1], Abdelkrim Ezaidi[1], Khawla Ramouch[1,2], Mohamed Ait Haddou[3]

[1] Geosciences, Environment and Geomatic Laboratory (GEG), Department of Geology, Faculty of Sciences, Ibnou Zohr University, B.P 8106, Agadir 80000, Morocco

[2] Geosciences, Geotourism, Natural Hazards and Remote Sensing Laboratory (L2GRT), Department of Geology, Faculty of Sciences Semlalia, B.P. 2390, Marrakech 40000, Morocco

[3] Department of Geography, Faculty of Human and Social Sciences, Ibn Tofail University, B.P 401, Kénitra 14000, Morocco

* Corresponding author's e-mail: ijjou.idoumskine@edu.uiz.ac.ma

ABSTRACT

This research sought to assess historically the urban expansion of Agadir city in Morocco within the 35-year timespan (1984–2019), and the influence of those changes on the regulating services of Agadir. It was achieved by applying support vector machine supervised (SVM) algorithm on each Landsat products to derive land use/land cover (LULC) maps. High accuracy assessment values were obtained for all Landsat classified maps. Spectral radiance model was exploited successfully to highlight the spatiotemporal changes of thermal behavior of city surfaces. Terrestrial carbon dynamics of Agadir LULC was evaluated by applying a process-based carbon model. The outcomes of this paper revealed an important urban expansion within the 35-year timespan with an important loss of vegetation and bare land. This urban evolution impacts the land surface temperature (LST) and caused carbon storage loss that contributes to local climate change. These findings could assist policy-makers to characterize a sustainable evolution of urban area, especially, to interpret how and where LULC changes might alter the dynamics of climate regulation and ecosystem services.

Keywords: supervised classification, Heat Island, carbon storage, InVEST model, ecosystem services.

INTRODUCTION

As stated in the Global Urbanization Forecasts presented by the United Nations in 2018, the worldwide demographic trends in cities will reach 68% by the end of 2050 with an accentuated growth in Asia and Africa [Chen 2024]. The rapid growth of populations and their activities increased the greenhouse gas concentration in the Earth's atmosphere [Qi et al. 2022]. In general, the unsustainable evolution of the human activities has a direct consequence on the ambient atmospheric conditions that affects the ecosystem services. Thus, scrutinizing the reciprocal impact of land use/land cover (LULC) transformations on micro-climate play a crucial role in accelerating transformations toward renewable development and mitigating Earth's atmosphere balance. Hence, two known parameters of the earth climate system are widely used to assess and monitor the effect of LULC changes namely, Land Surface Temperature (LST) and terrestrial carbon storage [Xiao et al. 2019].

LST is defined as the thermal behavior of a terrestrial surface and it is affected the anthropogenic activities that convert natural landscapes into impermeable surfaces [Adeyeri et al. 2024]. As listed by [Patel, Indraganti, and Jawarneh 2024], a variety of methodologies have been established and employed for extracting LST from remote sensing datasets, namely Physiologically

Equivalent Temperature (PET, universal thermal climate index (UTCI), and Surface Urban Heat Island Intensity (SUHII).

In fact, many scholarly inquiries have explored how changes in LULC patterns affect LST. [Orhan and Yakara 2016] investigated the correlation between alterations in vegetation and LST rates. Their study emphasized that agriculture activities in Konya, Turkey, contributed to about 5°C temperature increase between 1984 and 2014. [Nguemhe Fils et al. 2018] used multi-temporal Landsat scenes to conclude a continuous increase in linear link between LST and impervious areas in Douala Metropolis, Cameroon, from 1986 to 2016. [Sheik Mujabar 2019] revealed a significant difference in recorded temperature over an industrial city in Saudi Arabia, utilizing thermal infrared remote sensor (TIRS) data. He reported that the temperature in residential area ranges between 40°C and 50°C for summer, while in suburban areas it is moderate and in industrial area goes from 50°C to 55°C during the entire study period. In addition, he highlighted that temperatures more of than 60°C are recorded in the industrial facilities producing iron and steel.

Furthermore, the Integrated Valuation of Ecosystem Services and Tradeoffs (InVEST) algorithm deemed to be the simplest and most reliable tools for estimating the quantity of stored carbon [Verma et al. 2024]. The primary purpose of this model is to determine ecosystem carbon storage. It achieves this by multiplying mean density of carbon in reserves, namely living biomass (above and below ground), soil, litter and dead organic matter, for each LULC class with their corresponding areas, following the methodology proposed by [Mandle et al. 2016].

The research literature devoted to examining how urban growth affect ecosystem carbon reserves is extensive [W. Jiang et al. 2017; Verma et al. 2024]. Yet, only handful made use of the InVEST tool. The model was utilized by [Zhang et al. 2017] to monitor and assess the effects of shifts in land occupation on land-based carbon reservoirs in Uganda between 2006 and 2010. Outcomes indicated a reduction of approximately 29.1% in the sum total of carbon stocks across Uganda, averaging an annual decrease of about 7.3%. An integrated approach involving the Cellular Automata-Markov and InVEST tool was used by [Zhao et al. 2019] to evaluate the contribution of eco-friendly engineering to carbon sequestration in the Heihe River watershed in Northwest China. The developed methodology, with a relative error of 0.22%, predicts these circumstances will contribute to a significant upsurge in carbon preservation by 10.27 Tg from 2015 to 2029 within the studied area. [Hong et al. 2024] examined the carbon sequestration potential of urban forests in the Harbin-Changchun urban agglomeration from 2000 to 2020. The researchers emphasized a gradual increase in carbon sequestration capacity, particularly in large built-up areas.

In Morocco, studies have attempted to discern LULC impacts on LST [Garouani et al. 2021; Rahimi et al. 2021] and carbon safeguarding patterns [Mosaid et al. 2024; Moussadek et al. 2014] utilizing multi-temporal remote sensing data and focusing on the aspects related to urbanization. Neither of the aforementioned studies analyzed the impact of the land occupation on surface thermal and terrestrial carbon stocks conjunctly. Despite growing concerns regarding LULC changes and its effects on the global ecosystem and its sustainable development, the urban growth of cities in southern Morocco are less broadly studied. Thus, only few attempts have been made to study the LULC change of Agadir city in the Souss Massa region [Idoumskine et al. 2022].

Notably, this study represents the first comprehensive investigation into the environmental challenges facing Agadir city. This deficiency serves as the cornerstone of the conducted research, aiming to address the question of how LULC changes impact the local climate-related challenges by examining the correlation between both LST and terrestrial carbon dynamics and urban development patterns in Agadir city over the period spanning from 1984 to 2019. This examination is undertaken through a comprehensive approach that involves:

- extraction of LULC change data from Landsat products, utilizing the support vector machine SVM algorithm.
- evaluation of the spatial variations in Land Surface Temperature (LST) derived from the thermal bands of Landsat imagery.
- the identification of carbon stocks and sequestration levels to elucidate their dynamic responses to urbanization and land use transformations.

STUDY AREA

Agadir city is located on the Souss plateau at latitude 30° 25′ North and longitude 9° 36′ West along the Atlantic Ocean (Figure 1). The prevailing

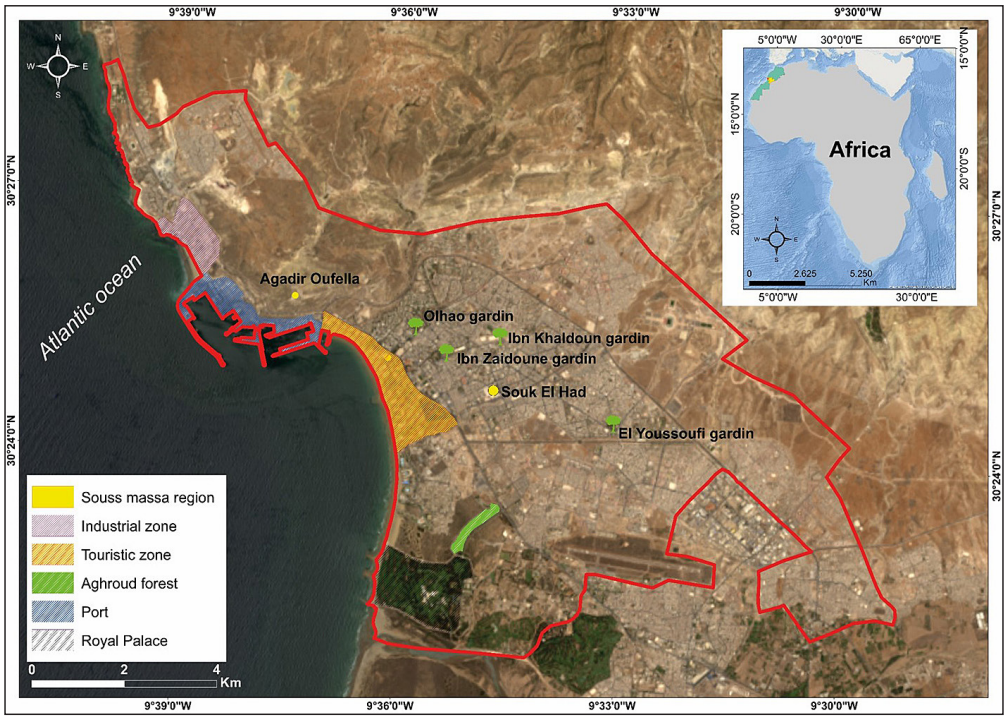

Figure 1. Localization of the Agadir city

climate is semi-arid with mainly Mediterranean oceanic influences characterized by a hot summer season (maximum temperature is recorded in July and August) and a cool winter season (January is the coldest month). The mean temperatures range between 20.04 and 26.04°C throughout the year with the highest in September and the lowest in January [WorldClim 2020]. With an mean yearly rainfall of 291.9 mm, the rain falls in Agadir for 39.4 days and the wettest month is December (60.7 mm) while the driest month is July (0.1 mm) [ABHSM n.d.]. According to [HCP 2014], Agadir contains 421 844 inhabitants spread across an area of 112 km². Historically, Agadir showed a significant demographic growth. Its population escalated from 110479 inhabitants in 1982 to 203000 inhabitants in 2006 [Brahim et al. 2021]. The total superficies of the city is subdivided in 13 districts and it includes residential areas, industrial areas, touristic areas and the port facilities [Agence Urbaine Agadir 2011]. The development economy of Agadir city is based on three sectors, namely fishing industry, tourism, as well as industrial and commercial.

The city is known as a tourist destination of excellence and a seaside resort of choice, the Agadir Regional Tourism Council (CRT) recorded an excess of 5,300.000 overnight stays in. In other hands, the developed infrastructures of the port of Agadir, the fishery sector (coastal, deep sea and artisanal) provides a total of 660 000 direct and indirect employments, and it produces 36% of the national added value. These statistics are increased with the installation of the first Halieutic pole in Morocco named 'Haliopolis'. The industrial zone of Agadir city employs more than 33 000 people and comprises more than 138 operational industrial units. The sector of commerce in Agadir is endowed with one of the largest urban markets in Morocco and Africa, the Souk El Had market covers an area of 9 ha, with more than 2 000 shops and 1 200 outlets and its visitors exceeds 50 000 in a normal day [HCP. 2020].

MATERIAL AND METHODOLOGY

Dataset

Three Landsat 5 scenes captured in 29th July 1984, 11th July 1994 and 4th June 2004, and two Landsat 8 images taken in 2nd July 2014 and 30th June 2019 were utilized within this paper. All images were obtained from Earth Explorer website provided by USGS website. Other Auxiliary data were employed, namely, shapefile of the administrative limits of the city, historical images of Google earth and climate data (air temperature and humidity) sourced from global climate and weather records [WorldClim 2020].

Methodology

As mentioned in the following sections, the process of this study will be described in three principal sections. The first one consists of preparing all Landsat scenes downloaded for the years 1984, 1994, 2004, 2014 and 2019. Then, the study field has been subseted from the corrected scenes using a shapefile in which the city is included. The second section is about estimating normalized indices – normalized difference vegetation index (NDVI) and normalized difference built up index (NDBI)) and developing the LULC change maps of the study years. SVM classifier was used, which requires Global positioning system (GPS) points as training samples for the classification process and others as ground truth (GT) for validation. The third section consists of retrieving the LST using thermal bands of the used Landsat products. Finally, the terrestrial carbon model developed by the InVEST was performed by considering the values of three carbon pools for each LULC class obtained from literature reviews. Figure 2 illustrates the research approach utilized in this study.

Data pre-processing

All Landsat scenes of the above-mentioned dates consisted of Level-One Terrain data (L1T), which are orthorectified and radiometrically calibrated [Cao, Gao, and Li 2024]. However, atmospheric conditions of each Landsat scene might be different since they were taken on different dates. Hence, fast line-of-sight atmospheric analysis of hypercubes (FLAASH) algorithm was executed on spectral bands of each satellite scene in order to enhance it atmospherically. Further, histogram equalization and resampling techniques have been performed to enhance the quality of the pre-processed images and to bring all images to the same pixel resolution, respectively.

Derivation of LULC maps and normalized indices

First, the obtained images from the pre-processing step are used to create LULC maps by applying the SVM algorithm as a supervised classifier using training samples obtained through field survey and observation of Google Earth archives. The SVM algorithm was chosen, because it performs better than other classical ones, such as maximum likelihood and minimum distance [Aydda et al. 2019]. As shown in Table 1, four LULC classifications were studied in this paper. Secondly, NDVI and NDBI were calculated. Both indices range among −1 and +1. Positive NDVI indicates high to moderate green surface, while they emphasize urbanized areas and bare lands covered by more than 5% of earthen material for NDBI. On the other hands, negative values of NDVI express the absence of vegetation and domination of constructed materials or water bodies, while they represent water bodies and areas with vegetation area for the NDBI [Idoumskine et al. 2022]. Each index was calculated using Eq. 1 and Eq. 2.

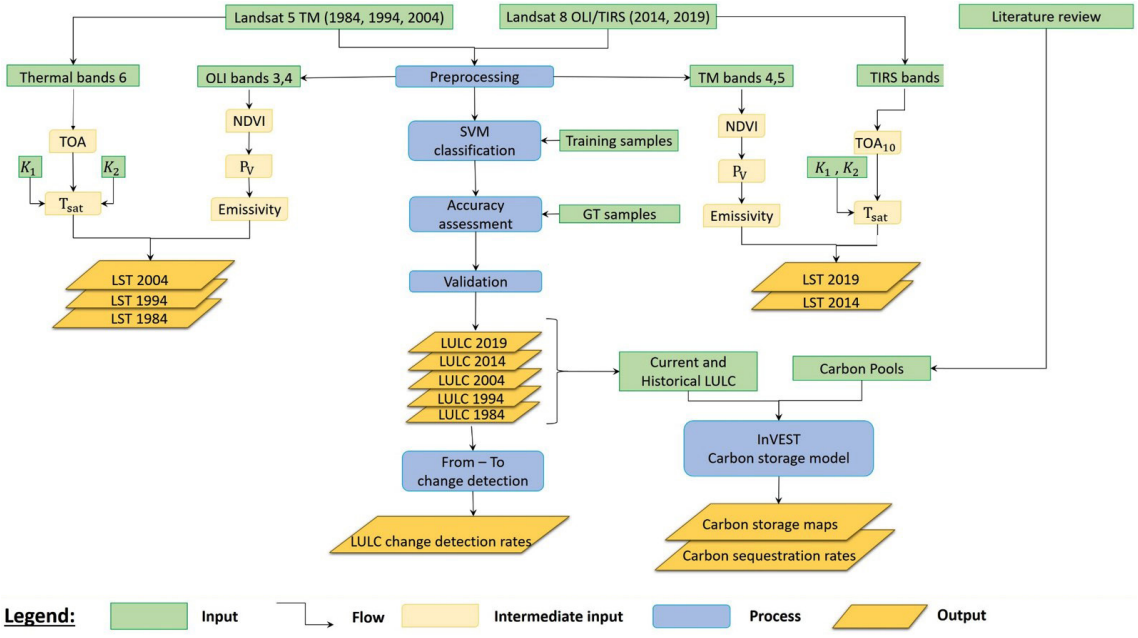

Figure 2. Workflow of the study

Table 1. LULC classes description

LULC Class	Descriptions
Bare land	Areas with no dominant vegetation cover or constructions, with the presence of earthen material.
Built-up land	Areas characterized by development intensity with domination of constructed materials
Vegetation	Areas dominated by canopy (≥4.5cm), shrub layer (1.5 cm to 2 cm) or grass.
Water	Areas with water surface, such as, swimming pools, rivers, lake oceans.

$$\text{NDVI} = \frac{Near\ infrared\ band - Red\ band}{Near\ infrared\ band + Red\ band} \quad (1)$$

$$\text{NDBI} = \frac{Short\ wave\ infrared\ bend - Near\ infrared\ band}{Short\ wave\ infrared\ bend - Near\ infrared\ band} \quad (2)$$

Retrieval of LST

In this part, TM and TIRS thermal bands are employed to extract the spatial variations of LST. First, top of atmospheric (TOA) spectral radiance was calculated using data available from metadata of each scene, by applying Eq. 3 for TM bands and Eq. (4) for TIRS bands [Y. Jiang et al. 2023]:

$$L_\lambda = \left(\frac{L_{\lambda MAx} - L_{\lambda MIN}}{Q_{CalMax}}\right) Q_{Cal} + L_{\lambda MIN} \quad (3)$$

$$L_{\lambda 1} = M_L \cdot Q_{cal} + A_L \quad (4)$$

where: L_λ and $L_{\lambda 1}$ are the TOP spectral brightness in W/ (m²/sr/mm) of TM and TIRS thermal bands, respectively. $L_{\lambda max}$ and $L_{\lambda min}$ are the highest value and the lowest value of spectral radiance, respectively. (Q_{CalMAX}) is the highest quantized calibrated information of pixel (Q_{Cal}). M_L and A_L are the radiance multiplier and the radiance supplement scaling element for each TIRS wavelength, respectively.

Subsequently, the effective factor at-satellite (brightness temperature) which is the sensor-measured apparent temperature of the surface was derived from TOA radiance by applying the inverted Planck's Law [Lin, Wei, and Guan 2024]. According to [Lin, Wei, and Guan 2024], the Eq. 5 was used for both Landsat products, by using the TOA spectral radiance obtained from the Eq. 3, and the TOA spectral radiance calculated using Eq. 4. The formula of conversion is as following:

$$T_{sat} = \left(\frac{K_2}{ln\left(\frac{K_1}{L_\lambda} + 1\right)}\right) - 273.15\ °C \quad (5)$$

where: the effective at-satellite temperature is expressed by T_{sat}, K_1 and K_2 are fixed values of the prelaunch calibration (Table 2), and the TOA spectral radiance is indicated by L_λ in W/(m²/r/μm). The T_{sat} is converted from the Kelvin (K) to Celsius (°C) by multiplying it by −273.15 [Avdan and Jovanovska 2016].

To retrieve the LST, land surface emissivity (LSE) was computed utilizing the emissivity described by [Sobrino et al. 2004] (Equation 6):

$$\varepsilon = m \cdot P_v + n \quad (6)$$

where: ε is the LSE, m and n are constant values, and P_v is the vegetation proportion, it was computed using least amount and the upper amount value of NDVI applying the Eq. (7).

$$P_v = \left[\frac{(\text{NDVI} - \text{NDVI}_{\min})}{(\text{NDVI}_{\max} - \text{NDVI}_{\min})}\right]^2 \quad (7)$$

Finally, LST was retrieved from the effective at-satellite temperature using the Eq. (8) [Du et al. 2014]:

$$\text{LST} = \left[\frac{T_{sat}}{1 + \left(\frac{\lambda \times T_{sat}}{\rho}\right) \times ln(\varepsilon)}\right] \quad (8)$$

where: T_{sat} indicates the effective at-satellite temperature, λ express the value of the wavelength emitted by the thermal bands, ρ is h×c/σ [Du et al. 2014], and ε is the LSE already calculated.

Terrestrial carbon change

Originated by the Natural Capital Project group, the InVEST carbon model is a GIS open tool. It provides information about the amounts of carbon stock in various terrestrial pools [Sharp et al. 2016]. The model requires two primary inputs, namely, LULC maps come out from the classification task and quantities of terrestrial carbon stocks in each carbon pool collected from literature reviews [Nel et al. 2022; Sharp et al. 2016] (Table 3). A diachronic analysis was done using the outputs

Table 2. Calibration constants

Parameter	Band 6	Band 10
K1 (W/m² srμm)	607.76	774.89
K2 (K)	1260.56	1321.08

of this model in order to assess the dynamics of the terrestrial carbon for all the study years.

Regression analysis

The extract point tool of ArcGIS was applied to generate testing value samples of LST, NDVI, NDBI and terrestrial carbon storage for each study year. Then, statistical analysis was carried out using scatter plots regression analysis of Microsoft Office Excel software for all five time-points, i.e., 1984, 1994, 2004, 2014 and 2019 to conduct an analysis of the interrelationships between LST, indices (NDBI and NDVI), and terrestrial carbon storage.

RESULTS

Classification and examination of LULC maps

Five LULC maps were generated from Landsat dataset, all with the maximum overall accuracy that could be obtained after performing the classification iteratively. The spatial expansion of each LULC class and its statistical changes over 35 years are displayed in Figure 3.

The built-up class exhibited a substantial growth with a net increase of 22.16 km², whereas bare land and vegetation cover witnessed a decrease in their areas with a net decrease of -25.17

Table 3. Quantities of terrestrial carbon pools of different LULC classes (Tg/C)

LULC Name	Carbon-aboveground	Carbon-belowground	Carbon-soil
Vegetation	31.20	1.10	18.67
Bare land	3.50	0.35	16.70
Built-up	3.00	0.60	13.50
Water	0.00	0.00	0.00

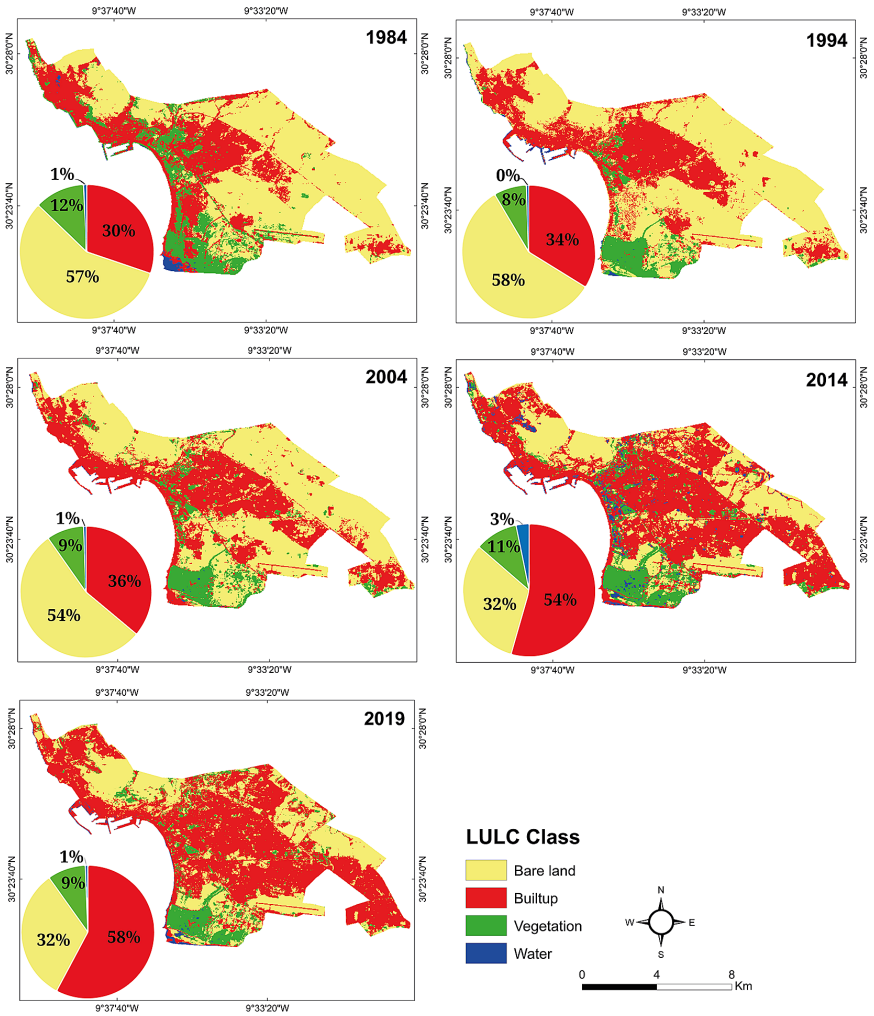

Figure 3. Spatial distribution and percentage of LULC classes for each study year

km² and -3.20 km², respectively. The water class showed a minor decrease of -0.18 km².

Evaluation of the final outputs of the classification process was determined through the confusion matrix and the Kappa coefficient. Both methods aim to visualize the performance of the classification by comparing its actual and predicted values of the target variables [Wan et al. 2024]. The total accuracy of the Landsat-derived LULC maps is given in Table 4.

Spatiotemporal pattern of the normalized indices

Figure 4 depicts the spatial distribution and the percentage of each NDVI class. The values

Table 4. Evaluation of the LULC maps

LULC classes	Landsat 5						Landsat 8			
	1984		1994		2004		2014		2019	
	Producer (%)	User (%)	Producer (%)	User (%)	Producer (%)	User (%)	Producer (%)	User (%)	Producer (%)	User (%)
Bare Land	98.80	96.96	99.94	67.35	99.0	97.18	100.00	98.21	99.15	99.59
Built-up	99.57	91.41	98.26	98.76	98.87	98.50	99.35	99.61	99.34	99.12
Vegetation	50.57	100.00	19.87	99.52	87.36	97.44	88.70	99.51	98.13	98.87
Water	100.00	100.00	100.00	99.35	99.93	99.93	100.00	99.72	99.72	99.92
Overall accuracy	98.60%		80.35%		99.02%		99.45%		99.70%	
Kappa coefficient	0.96		0.72		0.97		0.97		0.98	

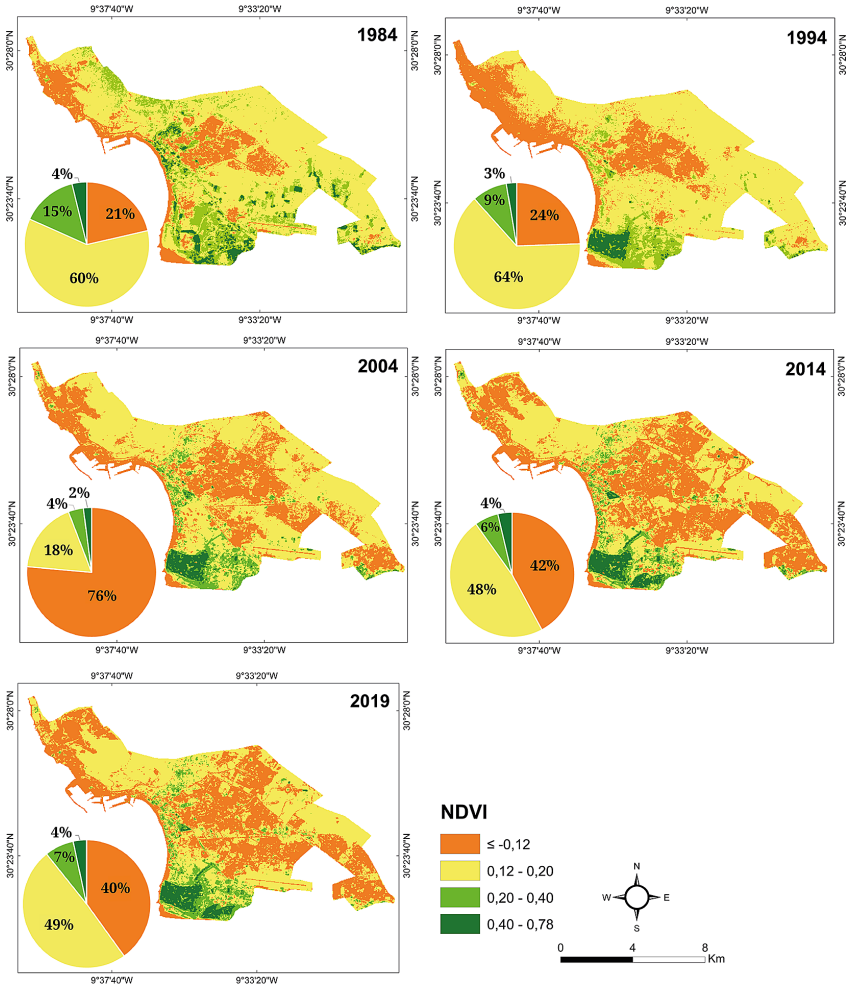

Figure 4. Spatial distribution and percentage of NDVI classes for each study year

were distributed between -0.21 and 0.36 in 1984, -0.05 and 0.37 in 1994, -0.39 and 0.52 in 2004, -0.26 and 0.78 in 2014, as well as -0.12 and 0.68 in 2019. Peak NDVI measurements are noted in both the western and southwest portions of the study area with a total surface of 16.03 km² in 1984, this total area decreased to 9.52 km² in 2019. The northeast, the central and the southeast sides of Agadir showed the minimum values of NDVI with a total area of 18.75 km² and 35.50 km² in 1984 and 2019, respectively. On the other hand, Figure 5 illustrates the spatial extent of NDBI and the area of each NDBI class in percentage. The NDBI included values from −0.31 to 0.20 in 1984, from −0.27 to 0.16 in 1994, from −0.47 to 0.23 in 2004, from −0.37 to 0.60 in 2014, and from −0.28 to 0.45 in 2019. Both the central and eastern areas of the city displayed elevated NDBI. These values witnessed an increase by 10.63 km² over the study analysis (from 59.82 in 1984 to 70.45 km² in 2019). In turn, low NDBI was identified in the northern part of the city. A decrease of 09.60 km² was highlighted, from 27.77 km² in 1984 to 18.18 km² in 2019.

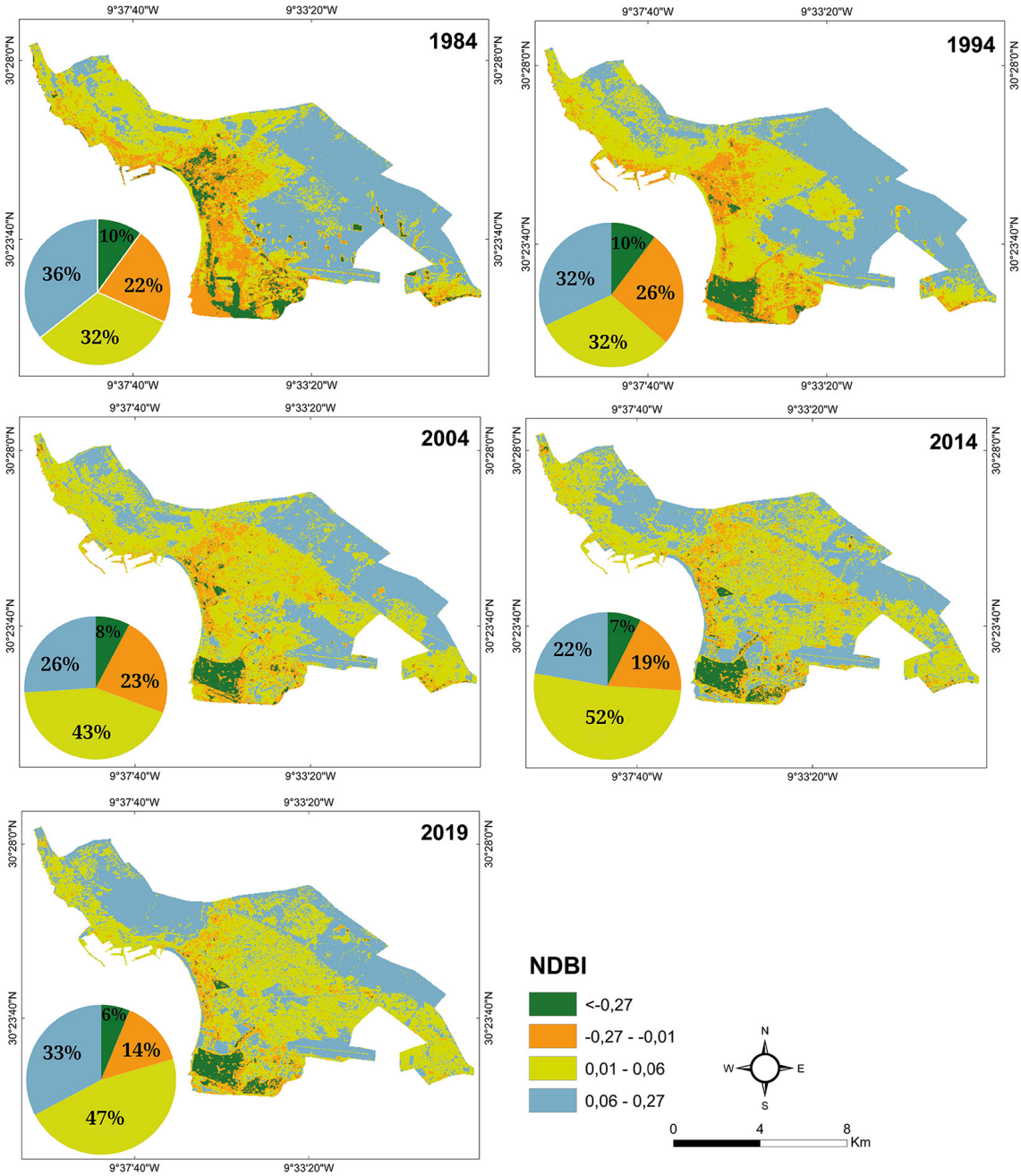

Figure 5. Spatial pattern and percentage of NDBI classes for the study years

LST retrieval

Figure 6 showcases the spatial distribution of LST captured across different time intervals throughout the research. The uppermost records of LST were recorded in 2004 and 2014 with a temperature of 40°C, while the temperatures less than 25°C were identified during 1994 and 2004 in large extent compared to other years. The results showed an average increase of temperature by 3.50°C for the period 1984–2014 and then a decrease by 2.60°C between 2014 and 2019.

Estimation of terrestrial carbon stocks and segregation

According to the output report generated by the model, the amount of carbon storage across Agadir LULC showed an overall stability (Figure 7). The highest rate of land-based carbon storage is reported in the aboveground biomass pool with an amount of 0.10 Tg C in 1984 and 3.33 Tg C in 2019 followed by the belowground biomass (0.001 to 0.8 Tg C) and soil organic. The mean carbon storage of the vegetation landscape in 1984 was estimated at

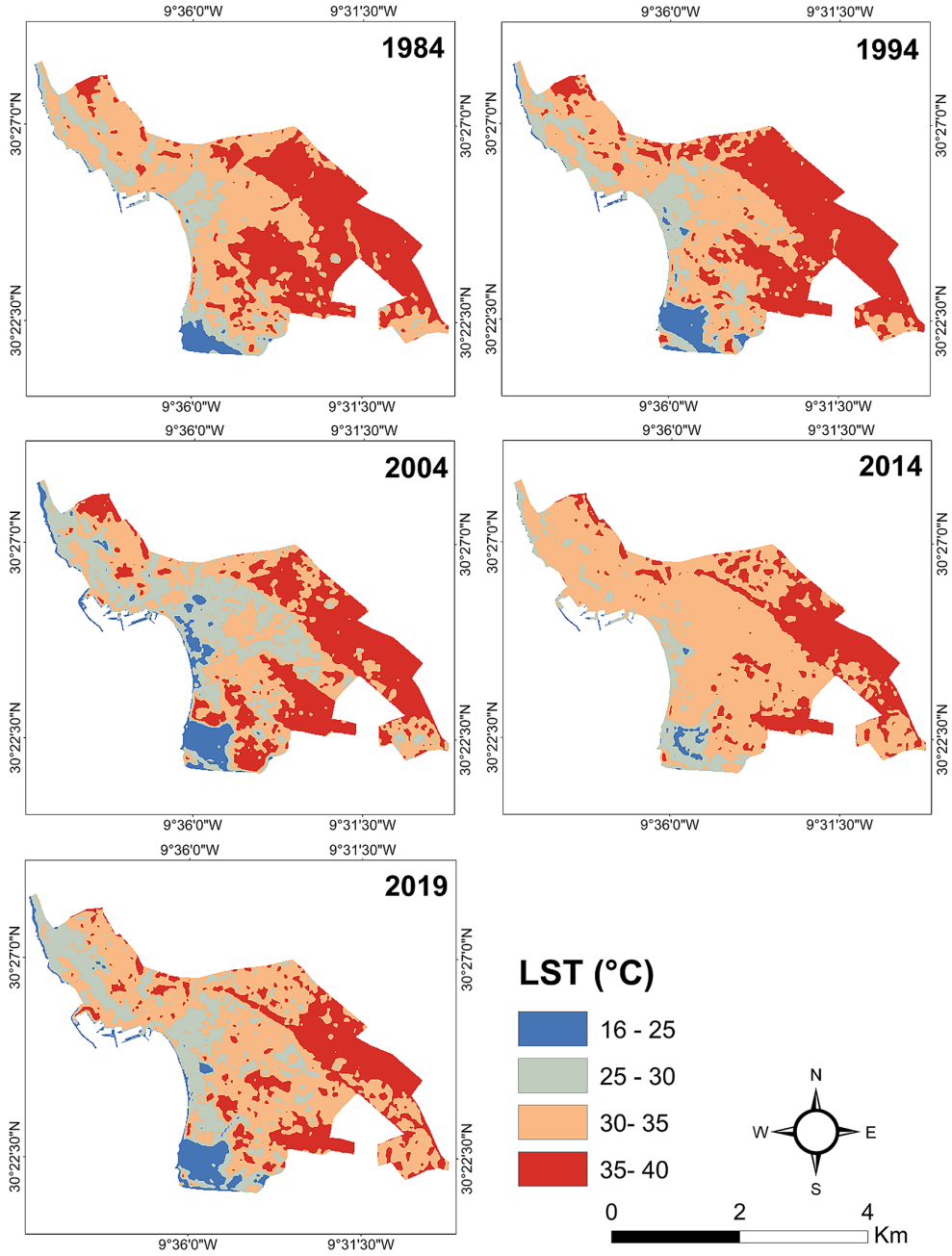

Figure 6. Spatial pattern of LST

1.88 Tg C, this amount will change to 4.34 Tg C, 4.08 Tg C, 4.59 Tg C, and 4.25 Tg C during 1994, 2004, 2014, and 2019, respectively. In contrast, the carbon storage of urban areas is reduced from 0.45 Tg C in 1984 to 0.13 Tg C in 2019, due to the significant conversion in LULC types and particularly the loss of vegetation cover. The values about the aboveground biomass during 2019 can be explained by the implantation of a significant quantity of the Florida palm trees over the city. The three pools illustrated positive values of stocking and sequestering terrestrial carbon during all the study years, except for the period 2004–2014 that recorded a negative value of sequestration (Figure 8).

DISCUSSION

LULC change detection

Post-classification analysis was carried out on each LULC map for the purpose of calculation the rates of changes of every class of LULC. Three intervals were chosen, namely, 1984–1994, 1994–2004, and 2004–2019. As per the results, in 1984, 59.67% of the total city area was covered by bare land. These surfaces decreased to 31.48% in 2019 in favor of the built-up class that witnessed a significant growth from 31.93% in 1998 to 57.38% in 2019. The green cover showed a low decrease between 1984 and 2019 (from 12.72% to 9.18%), while water class remained its total area between 0.81 and 3.22%.

Agadir LULC changes are due to two significant phenomena, the considerable demographic growth and its rapid economic development. The city witnessed an important urban growth of the city after the homologation of the new urban management plan of the city and the establishment of many urban subdivision plans in order to create new neighborhoods (Salam, Tikiouine, Al Houda, Hay Mohammadi) To address the requirements of the expanding population [Agence Urbaine Agadir 2011].

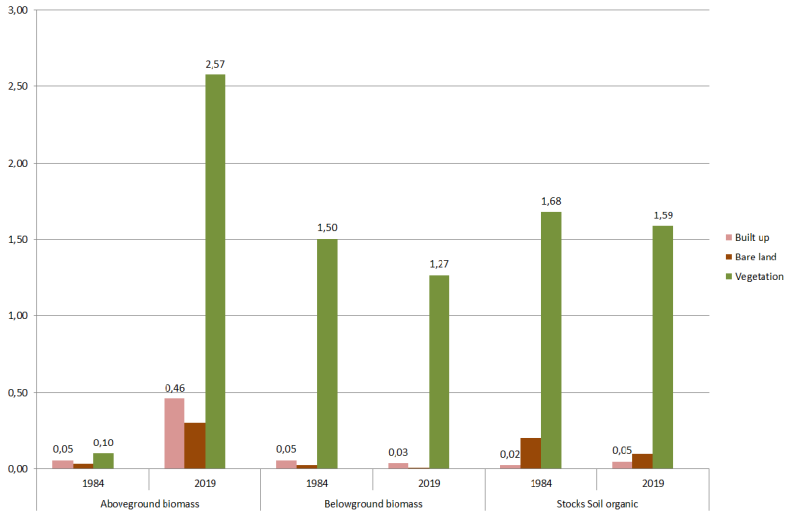

Figure 7. Terrestrial carbon (Tg C) in three land use classes

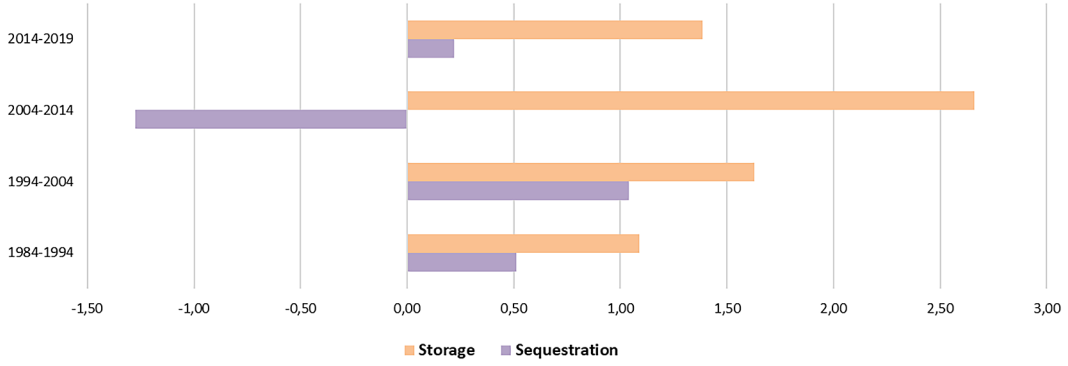

Figure 8. Total carbon stored and sequestered (Tg C)

The ERAC/Sud-Agadir establishment, now referred to as Groupe Al Omrane-Agadir is one of the leaders in housing and urban development that led the urban transformation of Agadir [Ben Attou 2003]. Between 1984 and 1994, ERAC-Sud-Agadir created 12366 completed units including 3753 houses, 400 commercial shops and 7895 residential lots, and 318 industrial lots. In addition, it realized 90488 residential units between 2004 and 2009. Furthermore, 900 ha of the total city area underwent transformation, resulting in the establishment of 19484 residential plots between 2007 and 2010; as part of the national program "cities without substandard housing" approved by the Moroccan government [Presentation of the Region | Souss Massa Region n.d.]. After the earthquake of 1960, significant efforts have been made to bring the shine re-develop the touristic sector along the coastline its natural landscapes. By the end of 1985, 46 hotels with about 2000 to 3000 bed capacity were built in the touristic zone, providing a considerable direct and indirect employment equal to 8000 workers. In addition, a completely new sector called Founty was built over 300 ha in the southernmost of the touristic zone towards the mouth of the Oued Souss. These numbers have continued to increase from 21586 beds in 2001 to 27904 in 2007. In 2019, the capacity of the touristic zone reached more than 40000 beds with an estimation of 550000 employment [HCP. 2020].

Other economic sectors led to the consumption of bare lands in the northernmost part of the city are the industrial activities and fishing industry. The industrial zone of 60 ha and Anza, that lies along the coast to the north of the city; are the two main locations of the industrial activities. Hence, many new residential areas were created next to the two industrial zones and the port in order to respond to the large flows of immigrants/workers to Agadir since the 1970s [Ben Attou and Semmoud 2015].

LULC change and its impact on LST change

The LST values within each LULC class were computed utilizing a statistic tool implemented in ArcGIS software. It was perceived that bare areas exhibited the highest temperatures, followed by urbanized regions. Specifically, the recorded maximum temperatures were 40.96°C in 2014 and 37.91°C in 2019, respectively. The presence of construction materials used in urban development can be seen because of the increase of social and economic needs of a population in exponential growth, therefore having positive regression coefficients of the LST-NDBI model (Figure 9). These results revealed that noticeable up surging of LST is recorded in the areas with high urban footprints, consistently with [Pannunzio et al. 2024] who linked the increasing LST to the areas that witnessed rapid urban growth or bare soil. With the analysis of [Min et al. 2019] who highlighted how the intensity and type of human activities that produced high emissions of pollutants can affect the urban micro-climate and create artificial heat sources.

By way of explanation, the green area and water body showed the lowest LST values with a minimum temperature equal to 20.75°C and 16.52°C, respectively, both recorded in 1984. Furthermore, an unfavorable association between LST and NDVI was identified for all the research time frame (Figure 10), in which the weaker LST were associated with higher values of NDVI. These values are due essentially to the presence of the eucalyptus forest of Aghroud nestled in the southwest side of the field study, covering 12 km² of the surface area, and the increase of urban vegetation especially in gardens, road network and private properties.

These outcomes are dependable with many authors such as [Iqbal and Ali 2022; Kumar et al. 2022] that evaluated the importance of vegetation partitions in regulating the thermal conditions of urbanized zones. [Lin, Wei, and Guan 2024] found that built-up area morphology causes changes in surface heat, so that its albedo decreases than green area, and causes a high LST. The solar radiation received by LULC types can alike lead to disparity in the LST recorded [Adeyeri et al. 2024]. The evapotranspiration of plants and water surfaces raise the atmospheric humidity and thereby abate the ambient temperature [Tao et al. 2024]

Effects of LULC change on terrestrial carbon dynamic

The outcome of carbon model analysis revealed the effects of the rapid growth of the study area on terrestrial carbon stocks, by calculating the quantity of sequestered or emitted carbon for each LULC class over the period 1984–2019.

Overall, the areas dominated by green cover or maintained with urban vegetation (coastal side) and zones with less road traffic with the

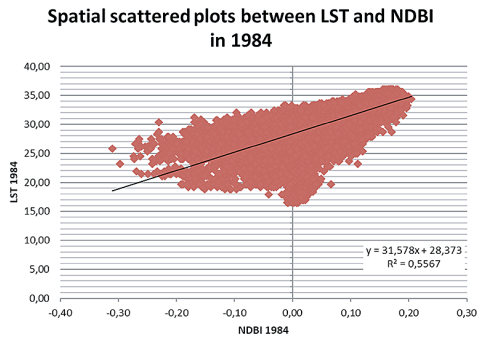

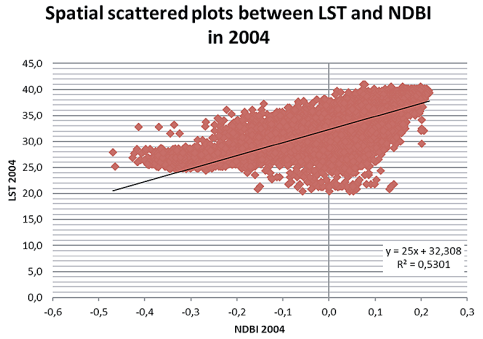

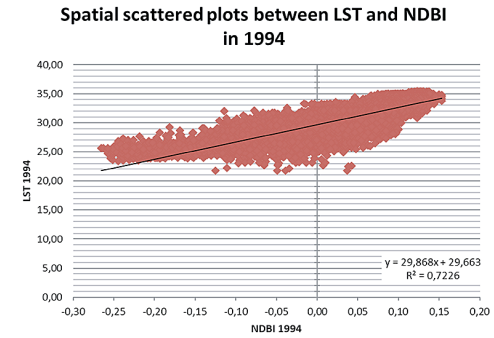

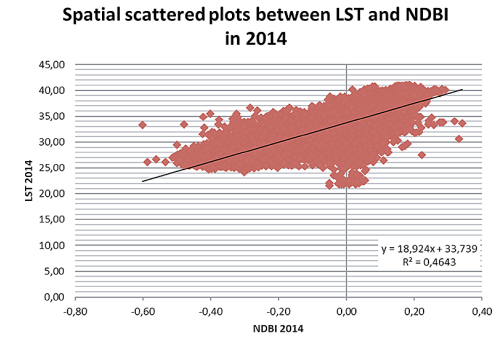

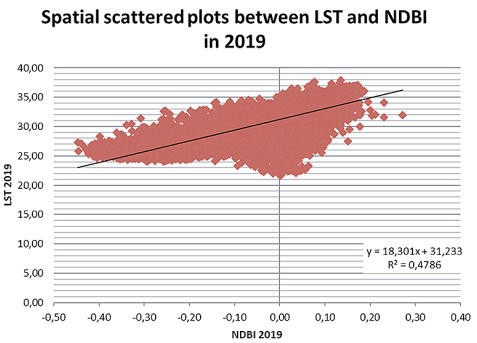

Figure 9. LST and NDBI correlation

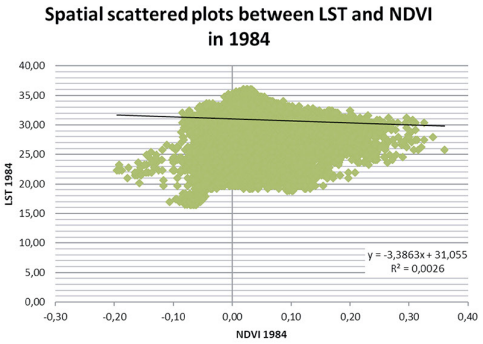

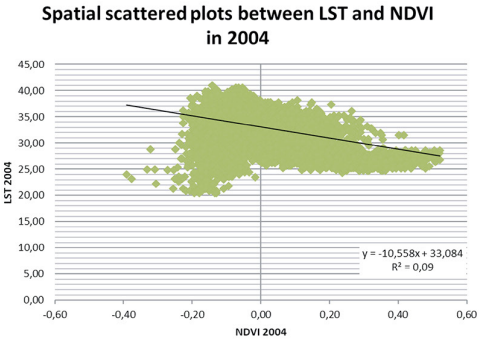

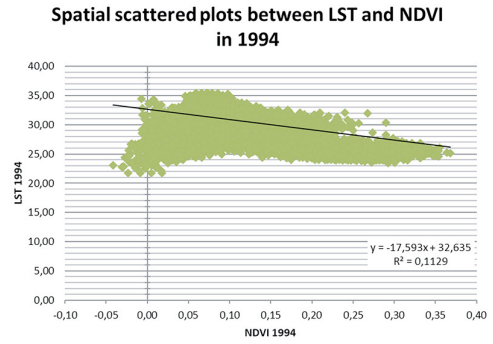

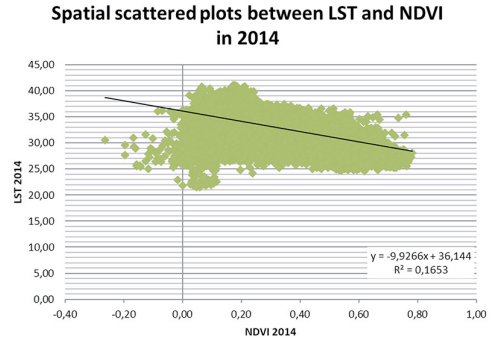

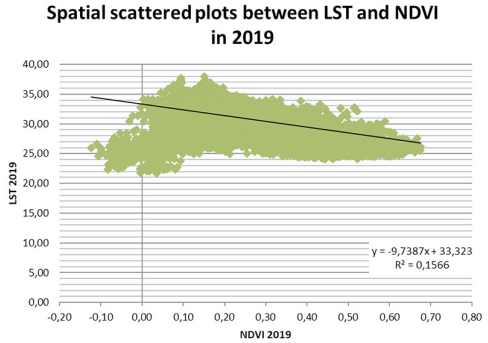

Figure 10. LST and NDVI correlation

Table 5. Amount of carbon sequestration

Year	1984–1994	1994–2004	2004–2014	2014–2019	1984–2019
Change in carbon (Tg of carbon)	0.050	0.103	- 0.127	0.021	0.050

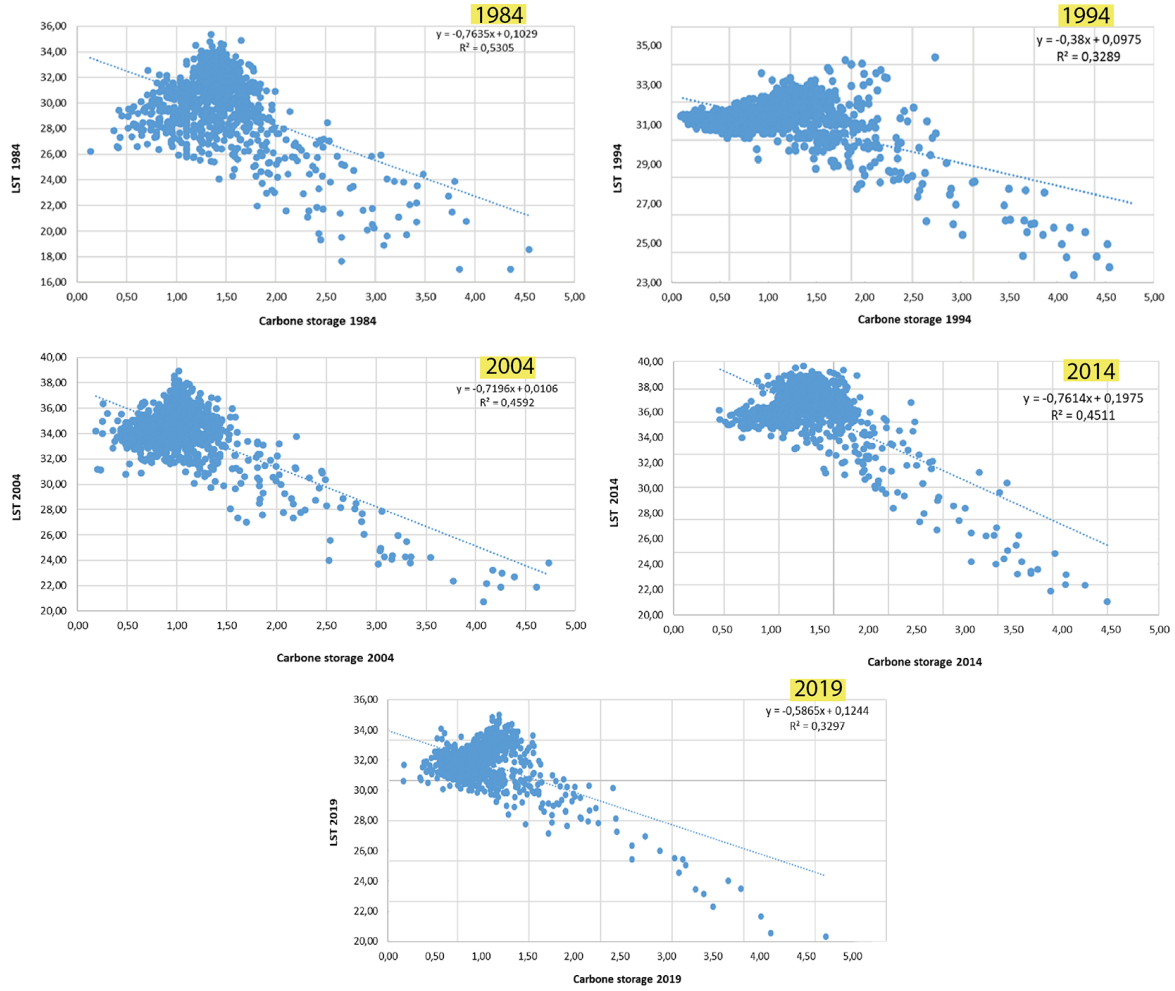

Figure 11. Correlation between LST and terrestrial carbon

presence of vegetation cover (Identified notably in the northeast and southwest sectors of the region studied) showed high levels of capacity of sequestration. On the other hands, a loss of 0.127 Tg of carbon was observed in dense urbanized areas located essentially at the central part of the city during the period 2004–2014.

Several studies discussed the link between LULC dynamic and terrestrial carbon over the world are confirming the finding of this analysis, citing for example [Nguemhe Fils et al. 2018], [Kusi et al. 2020] and [Piyathilake et al. 2022].

Moreover, Table 5 shows the amount of carbon sequestration for the same period. The maximum capacity of carbon sequestration was estimated to be 0.103 Tg C and it was recorded for the period 1994–2004, whilst the maximum carbon loss recorded in the converted area (from vegetation to built-up area) reaches to -0.127 Mg C during the period 2004–2014.

Terrestrial carbon dynamic and its relationship with LST

Figure 11 highlights the regression analysis of LST distribution in relation with the terrestrial carbon. Numerous studies have examined the correlation between high temperature and global carbon cycle, the key measure of ecosystem mechanism and a critical intersection between the terrestrial biosphere and the Earth's climate [Xiao et al. 2019]. Cross-validation output showed that

LST values are negatively correlated with terrestrial carbon storage. Thus, the increases of anthropogenic interventions (energy consumption, urbanization, economic activities) and the alarming decline in terrestrial carbon pools such as vegetation coverage will massively increase the amount of greenhouse gas released to the atmosphere. Especially the carbon dioxide (CO_2) that affects the LST, harming human wellness, and reducing the climate sustainability of the city. This finding is similar to [Chaddad et al. 2022] and [Chalchissa and Kuris 2024] who devoted to quantifying the consequences of LULC alterations on ground temperature and carbon dynamics.

CONCLUSIONS

Due to the increase in anthropogenic activities over the last few decades, the composition of Earth's biosphere has undergone significant changes. The aim of this study was to discern and evaluate the LULC changes and its impact on the spatiotemporal dynamics of terrestrial carbon stocks and thermal characteristics of Agadir city, utilizing multi-temporal Landsat datasets spanning from 1984 to 2019.

The results illustrate a notable conversion of vegetated and bare lands into urbanized areas. This urban expansion demonstrates a significant linear correlation with LST records, indicating that the weather conditions of this city are becoming more extreme over time. Additionally, this study highlights the impact of urbanization on the physical characteristics of the land surface, contributing to a decline in terrestrial carbon stocks.

The obtained findings indicate that improving vegetation areas has the potential to reduce LST while also offering an opportunity to sequester carbon, emphasizing the imperative of increasing green spaces and implementing appropriate measures to promote afforestation, particularly in barren land areas.

Hence, the findings offer valuable insights for guiding future research efforts on the impact of various policies on LULC changes in semi-arid regions. By utilizing high-resolution data and advanced algorithms, future studies could delve deeper into monitoring the effects of the growing trend in settlement areas on local environmental health and vulnerability. This would enable informed decision-making and facilitate proactive measures to address emerging challenges.

REFERENCES

1. ABHSM. Situation Hydrologique. http://www.abhsm.ma/index.php/situation-hydrologique (April 8, 2019).
2. Adeyeri, Oluwafemi E. et al. 2024. Land surface dynamics and meteorological forcings modulate land surface temperature characteristics. Sustainable Cities and Society 101(November 2023): 105072. https://doi.org/10.1016/j.scs.2023.105072.
3. Agence Urbaine Agadir. 2011. Plan D'amenagement d'Agadir.
4. Avdan, U., Gordana Jovanovska G.. 2016. Algorithm for automated mapping of land surface temperature using LANDSAT 8 satellite data. Journal of Sensors, vol. 16, 8 pages, Article ID 1480307.
5. Aydda, Ali, Omar F. Althuwaynee, Ahmed Algouti, and Abdellah Algouti. 2019. Evolution of Sand Encroachment using supervised classification of landsat data during the period 1987–2011 in a part of Laâyoune-Tarfaya basin of Morocco. Geocarto International, 34(13): 1514–29. http://dx.doi.org/10.1080/10106049.2018.1493154.
6. M. Ben Attou, Bouziane S. 2015. Agadir et Ses Espaces Ruraux Sous Influence Urbaine : Stratégies d'acteurs et Nouveaux Lieux Mondialisés.Cahiers de géographie du Québec 58(163): 93.
7. Ben Attou, Mohamed. 2003. "Agadir gestion urbaine, stratégies d'acteurs et rôle de la société civile : urbanisme opérationnel ou urbanisme de fait?" Insaniyat (22): 37–58. http://journals.openedition.org/insaniyat/6881 (April 10, 2023).
8. Kidou, B., Askassay K., Elamrani A., Hasna T., Guedil K., Atiki N. 2021. population urbaine et consommation d'eau dans une region semi-aride: cas du grand Agadir (Maroc). Geomaghreb 17: 58–72.
9. Cao, Xiaomin, Xiaohong Gao, and Runxiang Li. 2024. Heliyon research on the spatial temporary evolution of urban expansion in xining city and its surrounding areas based on landsat time. Heliyon 10(3): e24846. https://doi.org/10.1016/j.heliyon.2024.e24846.
10. Chaddad, F. et al. 2022. Impact of mining-induced deforestation on soil surface temperature and carbon stocks: a case study using remote sensing in the amazon rainforest. Journal of South American Earth Sciences 119(2021): 103983.
11. Chalchissa, F.B., Kuris B.K. 2024. Modelling soil organic carbon dynamics under extreme climate and land use and land cover changes in western oromia regional state, Ethiopia. Journal of environmental management 350(August 2023): 119598. https://doi.org/10.1016/j.jenvman.2023.119598.
12. Chen, Meiguirong. 2024. Impacts of Urbanization and Climate Change on Ecosystems in Asia: Challenges and Conservation Strategies. In: Third International

Conference on Biological Engineering and Medical Science (ICBioMed2023), SPIE, 1063–67.

13. Du, Chen et al. 2014. Split-window algorithm for estimating land surface temperature from Landsat 8 TIRS data. International Geoscience and Remote Sensing Symposium (IGARSS) (Ldcm): 3578–81.
14. Manal El G., Amyay M., Lahrach A., Oulidi H.J. 2021. Land surface temperature in response to land use/cover change based on remote sensing data and GIS techniques: application to saïss plain, Morocco. Journal of Ecological Engineering 22(7): 100–112.
15. HCP. 2014. Recensement général de la population et de l'habitat 2014 (RGPH2014). Recensement général de la population et de l'habitat. https://rgph2014.hcp.ma/downloads/Resultats-RGPH-2014_t18649.html (December 26, 2019).
16. HCP. 2020. Monographie de La Région de Souss Massa. Agadir, Maroc.
17. Hong, W. et al. 2024. Spatiotemporal changes in urban forest carbon sequestration capacity and its potential drivers in an urban agglomeration: implications for urban CO 2 emission mitigation under China' s rapid urbanization. Ecological Indicators 159(October 2023): 111601. https://doi.org/10.1016/j.ecolind.2024.111601.
18. Idoumskine, I., Aydda A., Ezaidi A., Omar F. Althuwaynee. 2022. Assessing land use/land cover change using multitemporal landsat data in Agadir City (Morocco): 337–50.
19. Benazeer B., Ali. M. 2022. Estimation of spatiotemporal air temperature from satellite based LST under semi-arid to arid environment in Peshawar Basin, Northwest Pakistan. Advances in Space Research 70(4): 961–75.
20. Jiang, W. et al. 2017. Modelling the potential impacts of urban ecosystem changes on carbon storage under different scenarios by linking the CLUE-S and the InVEST models. Ecological Modelling 345: 30–40. http://dx.doi.org/10.1016/j.ecolmodel.2016.12.002.
21. Jiang, Y., Lin W., Di Xu, Dan Xu. 2023. Spatio-temporal variation of the relationship between air pollutants and land surface temperature in the Yangtze river delta urban agglomeration, China. Sustainable Cities and Society 91(December 2021).
22. Kumar, B. Pradeep, K. Raghu Babu, B.N. Anusha, Rajasekhar. M. 2022. Geo-environmental monitoring and assessment of land degradation and desertification in the semi-arid regions using Landsat 8 OLI / TIRS, LST, and NDVI approach. Environmental Challenges 8(December 2021).
23. Kusi, K.K., Khattabi A., Nadia Mhammdi, Lahssini S. 2020. Prospective evaluation of the impact of land use change on ecosystem services in the Ourika watershed, Morocco. Land Use Policy 97(July 2019): 104796. https://doi.org/10.1016/j.landusepol.2020.104796.
24. Lin, J., Wei K., Guan Z. 2024. Exploring the connection between morphological characteristic of built-up areas and surface heat islands based on MSPA. Urban Climate 53(October 2023): 101764. https://doi.org/10.1016/j.uclim.2023.101764.
25. Mandle, L. et al. 2016. OPAL: An open-source software tool for integrating biodiversity and ecosystem services into impact assessment and mitigation decisions. Environmental Modelling and Software 84: 121–33. http://dx.doi.org/10.1016/j.envsoft.2016.06.008.
26. Min, M. et al. 2019. Spatial distribution and driving force analysis of urban heat island effect based on raster data: a case study of the Nanjing metropolitan area, China. Sustainable Cities and Society 50(December 2018): 101637. https://doi.org/10.1016/j.scs.2019.101637.
27. Hassan M. et al. 2024. Improved soil carbon stock spatial prediction in a mediterranean soil erosion site through robust machine learning techniques. Environmental Monitoring and Assessment 196(2): 130. https://doi.org/10.1007/s10661-024-12294-x.
28. Moussadek, R. et al. 2014. Tillage system affects soil organic carbon storage and quality in central Morocco. Applied and Environmental Soil Science 2014.
29. Nel, L. et al. 2022. InVEST Soil carbon stock modelling of agricultural landscapes as an ecosystem service indicator. Sustainability (Switzerland) 14(16): 1–19.
30. SC Nguemhe Fils et al. 2018. TM/ETM+/LDCM images for studying land surface temperature (LST) interplay with impervious surfaces changes over time within the Douala metropolis, Cameroon. Journal of the Indian Society of Remote Sensing 46(1): 131–43.
31. Orhan, O., Yakara M. 2016. Investigating land surface temperature changes using Landsat data in Konya, Turkey. In: International Archives of the Photogrammetry, Remote Sensing and Spatial Information Sciences - ISPRS Archives, 285–89.
32. Pannunzio, M. et al. 2024. Remote sensing applications: society and environment impacts of urban landscape pattern changes on land surface temperature in southeast Brazil. Remote Sensing Applications: Society and Environment 33(January): 101142. https://doi.org/10.1016/j.rsase.2024.101142.
33. Patel, S., Indraganti M., Jawarneh Rana N. 2024. A comprehensive systematic review: impact of land use/ land cover (LULC) on land surface temperatures (LST) and outdoor thermal comfort. Building and Environment 249(August 2023): 111130.
34. Piyathilake, I.D.U.H., Udayakumara E. P.N., Ranaweera L.V., Gunatilake S.K. 2022. Modeling predictive assessment of carbon storage using InVEST model in uva province, Sri Lanka. Modeling Earth Systems and Environment 8(2): 2213–23.

https://doi.org/10.1007/s40808-021-01207-3.

35. Presentation of the Region | Souss Massa Region. https://www.soussmassa.ma/en/presentation-region (April 8, 2023).
36. Qi, Xiao lian et al. 2022. Effects of climate change, coal mining and grazing on vegetation dynamics in the mountain permafrost regions. Ecological Informatics 69: 101684.
37. Rahimi, A. et al. 2021. Land surface temperature responses to land use land cover dynamics (District of Taroudant, Morocco). In Biology and Life Sciences Forum, MDPI, 28.
38. Sharp, R. et al. 2016. InVEST User's Guide. The Natural Capital Project. Stanford university, university of Minnesota, the nature conservancy, and World Wildlife Fund: 371.
39. Sheik Mujabar, P. 2019. Spatial-temporal variation of land surface temperature of jubail industrial city, saudi arabia due to seasonal effect by using thermal infrared remote sensor (TIRS) satellite data. Journal of African Earth Sciences 155(March 2019): 54–63. https://doi.org/10.1016/j.jafrearsci.2019.03.008.
40. Sobrino, J.A. et al. 2004. Single-channel and two-channel methods for land surface temperature retrieval from DAIS data and its application to the barrax site. International Journal of Remote Sensing 25(1): 215–30.
41. Tao, S., Song L., Zhao G., Zhao L. 2024. Simulation and assessment of daily evapotranspiration in the Heihe river basin over a long time series based on TSEB-SM. Remote Sensing 16(3): 462.
42. Verma, P., Siddiqui A.R., Mourya N.K., Devi A.R. 2024. Forest carbon sequestration mapping and economic quantification infusing MLPnn-Markov Chain and InVEST carbon model in askot wildlife sanctuary, Western Himalaya. Ecological Informatics 79(August 2023): 102428. https://doi.org/10.1016/j.ecoinf.2023.102428.
43. Wan, C. et al. 2024. DBPF-Net: dual-branch structural feature extraction reinforcement network for ocular surface disease image classification. Frontiers in Medicine 10: 1309097.
44. WorldClim. 2020. Global climate and weather data. global climate and weather data. https://www.worldclim.org/data/index.html (February 18, 2023).
45. Xiao, J. et al. 2019. Remote sensing of the terrestrial carbon cycle: a review of advances over 50 years. Remote Sensing of Environment 233(August).
46. Zhang, F. et al. 2017. Impacts of land use/cover change on terrestrial carbon stocks in Uganda. Physics and Chemistry of the Earth 101: 195–203. http://dx.doi.org/10.1016/j.pce.2017.03.005.
47. Zhao, M. et al. 2019. Assessing the effects of ecological engineering on carbon storage by linking the CA-Markov and InVEST models. Ecological Indicators 98(September 2018): 29–38. https://doi.org/10.1016/j.ecolind.2018.10.052.